ELSEVIER

Journal of Photochemistry and Photobiology A: Chemistry 141 (2001) 47–56

Journal of Photochemistry and Photobiology A:Chemistry

www.elsevier.nl/locate/jphotochem

Photochemical and photocatalytic degradation of an indigoid dye: a case study of acid blue 74 (AB74)

Catherine Galindo [a,*], Patrice Jacques [b], André Kalt [a]

[a] *Laboratoire de Chimie Textile, Ecole Nationale Supérieure de Chimie de Mulhouse, 3 rue A. Werner F 68093 Mulhouse, France*
[b] *Département de Photochimie Générale, UMR CNRS No. 7525, Ecole Nationale Supérieure de Chimie de Mulhouse, 3 rue A. Werner F 68093 Mulhouse, France*

Received 25 January 2001; received in revised form 28 March 2001; accepted 30 March 2001

Abstract

A detailed investigation of the photochemical and photocatalytic degradations of the indigoid dye AB74 is presented. H_2O_2 and C-UV light have negligible effect when they are used on their own. However, joint UV/H_2O_2 treatment more efficiently decomposes this organic compound. Surprisingly, reaction order depends strongly on the initial dye concentration. On the other hand, ^{1}H NMR analysis reveals that the original dye is first converted into isatinsulfonic acid, then into aliphatic acids. Under band gap excitation of semiconductors, AB74 undergoes irreversible oxidation too. The photodegradation kinetics, on various catalysts, are discussed in term of the Langmuir–Hinshelwood model. ^{1}H NMR, UV–VIS and FTIR spectroscopic techniques provide an insight into the nature of the photoproducts. It was possible then to present a more complete degradation mechanism than supposed until now. © 2001 Published by Elsevier Science B.V.

Keywords: Indigoid dye; UV/H_2O_2 process; Photocatalysis; Kinetics

1. Introductions

The textile industry consumes considerable amounts of water during the dyeing and finishing operations. Dyes are extensively used and hence wastewaters discharged in rivers or public sewage treatment plants are highly contaminated. Now, colored water is unattractive and generates more and more complaints. Moreover, concerns are expressed about the potential toxicity of dyes and of their precursors. Environmental pollution by organic dyes also sets a severe ecological problem, which is increased by the fact that most of them are difficult to degrade using standard biological methods [1]. For the removal of such recalcitrant pollutants, traditional physical techniques (adsorption on activated carbon, ultrafiltration, reverse osmosis ...) can generally be used efficiently. Nevertheless, they are non-destructive, since they just transfer organic matter from water to sludge. Consequently, regeneration of the adsorbent materials and post-treatment of solid wastes, which are expensive operations, are needed [2].

Recently, there has been considerable interest in the utilization of advanced oxidation processes (AOPs) for the destruction of organic compounds in contaminated water [3,4]. Two of them seem very promising: the UV/oxidation process, which involves ultraviolet irradiation in conjunction with hydrogen peroxide and the heterogeneous photocatalysis UV/TiO_2. The key advantage of the former is its inherent destructive nature: it does not involve mass transfer; it can be carried out under ambient conditions and may lead to complete mineralization of organic carbon into CO_2 [5]. Moreover, photocatalytic process is receiving increasing attention because of its low cost when using sunlight as the source of irradiation.

In the present paper, we examine the degradation of the indigoid dye, acid blue 74 (AB74), commonly named Indigo Carmine, by these techniques. Both kinetic and mechanistic aspects were investigated. AB74 was chosen, since it has been the topic of only a few articles, and the nature of by-products remains a matter of conjecture [6,7].

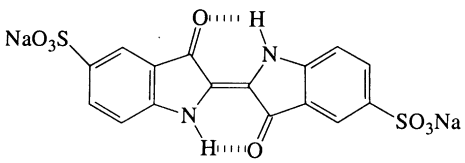

The dye AB74

* Corresponding author. Fax: +33-89336805.
E-mail address: c.galindo@univ.mulhouse.fr (C. Galindo).

1010-6030/01/$ – see front matter © 2001 Published by Elsevier Science B.V.
PII: S1010-6030(01)00435-X

2. Experimental section

2.1. Reagents

The indigoid dye CI acid blue 74 (AB74) and isatinsulfonic acid sodium salt are Aldrich products. They were used without further purification. Solutions were prepared by dissolving a defined quantity of these compounds in distilled water. Hydrogen peroxide (30% w/w) and zinc oxide were purchased from Prolabo. Titanium dioxide was supplied by Degussa (P25), by Millenium (Tiona PC 500, Tiona PC 100) and by Dupont de Nemours (R900, TC4). Characteristic of theses oxides are collected in Table 1.

2.2. Photoreactors and light sources

For the UV and UV/H_2O_2 processes, irradiations were performed in a batch photoreactor of 500 ml in volume, fitted with a 15 W low-pressure mercury lamp (Philips, emission: 253.7 nm). The radiant flux of this lamp was determined by means of a chemical actinometer: hydrogen peroxide. The actinometer was irradiated under conditions similar to those of the photoreaction used. This eliminated the need to make corrections due to the reflectance and non uniformity of the incident light beam. The incident photon flux, called P_0, was estimated at 2.7×10^{-6} einstein s^{-1}. For the UV/catalyst process, irradiations were performed with a 18 W black-light mercury lamp (Philips, $\lambda > 310$ nm) in the same reactor.

In order to study the influence of air, solutions were photolysed in quartz vessels (3.1 ml). De-aerated conditions were achieved by bubbling nitrogen into the solution for 20 min before irradiation and by maintaining a gaseous flow above the cell during the treatment.

2.3. Procedures

Solutions with the desired concentration in dye and the load of TiO_2, ZnO or H_2O_2 were fed into the reactor. The aqueous solutions were magnetically stirred. The pH of the solution was adjusted using dilute nitric acid or aqueous sodium hydroxide solutions. After 30 min of premixing, the lamp was switched on to initiate the reaction. At regular time intervals, samples were taken and, when appropriate, filtrated on a 0.45 μm syringe filter.

Table 1
Characteristics of TiO_2[a]

TiO_2	Composition	Specific area ($m^2\,g^{-1}$)
P25	Anatase: 80% Rutile: 20%	50
Tiona PC 500	Anatase ≥99%	250
Tiona PC 100	Anatase ≥99%	Between 80 and 100
R900	Rutile ≥99%	NC
TC4	Rutile ≥99%	NC

[a] NC: non communicated by the producer.

The adsorption isotherms were obtained by prolonged agitation of the suspensions, followed by a spectrophotometric measurement of the dye remaining in the solution. All isotherm measurements were made in the dark.

2.4. Analytical control

The efficiency of the process was evaluated by monitoring the dye discoloration at 609 nm, which corresponds to the maximum absorption wavelength, using a Kontron Uvikon 943 spectrophotometer. The total organic carbon (TOC) reduction was measured with a Beckman Tocamaster carbon analyzer (model 915-B). NMR spectra were recorded on a BRUCKER AC 250.13 MHz spectrometer.

After irradiation, the solution was evaporated under reduced pressure. The residue was esterified using thionyl chloride and methanol and finally analyzed by GC/MS on an analytical mass spectrometer fitted with a Hewlett-Packard 5890 Series II GC apparatus containing a capillary column (25 m long, 0.15 mm in width). A temperature gradient was used in the separation. The temperature was maintained at 80°C for 3 min, then increased to 310°C at a rate of 3.5°C min^{-1}.

For FTIR analysis, AB74 (1.2×10^{-4} M) was adsorbed on titanium dioxide particules (7.5 g l^{-1}). The residue was dried at room temperature. A wafer was made by pressing 30 mg of powder in a laboratory press at 7.5 bars. It was then irradiated using the black-light lamp. FTIR spectra were periodically recorded using a Nicolet 710 spectrometer. Absorbance spectra were measured in the 1000–1900 cm^{-1} region with a resolution of 4 cm^{-1}. Titanium dioxide was used as a background reference.

3. Results and discussions

3.1. UV (253.7 nm) alone

When C-UV light is applied only in the presence of oxygen (without photocatalysts or hydroxyl radical precursors), discoloration degrees are observed. With ε_{AB74} and ϕ_{AB74} the extinction coefficient and the quantum yield, the rate of photolysis is given by *the* following equation, where the index *i* refers to species (except AB74) that absorb radiation at 253.7 nm, i.e. breakdown products, P_0 to the incident photon flux, and *l* to the thickness of the solution.

$$-\frac{\mathrm{d}[\mathrm{AB74}]}{\mathrm{d}t} = P_0 \Phi_{\mathrm{AB74}} \frac{\varepsilon_{\mathrm{AB74}}[\mathrm{AB74}]}{\varepsilon_{\mathrm{AB74}}[\mathrm{AB74}] + \sum_i \varepsilon_i[i]} \times \left[1 - \exp\left(-2.3l\left(\sum_i \varepsilon_i[i] + \varepsilon_{\mathrm{AB74}}[\mathrm{AB74}]\right)\right)\right] \quad (1)$$

Eq. (1) can be simplified because the exponential term is negligibly small, so that well in excess of 99% of the light reaching the reactor is absorbed within it. On the other hand, at the beginning of the treatment, the contribution of breakdown products can be neglected, which leads to

$$-\frac{\mathrm{d[AB74]}}{\mathrm{d}t} = -r_{\mathrm{UV}} = P_0 \Phi_{\mathrm{AB74}} \quad (2)$$

This system can be integrated using the experimental concentration — time data. The average quantum yield value is 2.2×10^{-3}. This rather low value indicates that the dye dissipates excitation energy via non-reactive pathways with high efficiency.

Moreover, from the mechanistic point of view, the involvement of singlet oxygen can be assumed, as it was proved for the non-sulfonated dye in organic solution under UV or visible light [8]. Indeed, the photostability of AB74 depends on the presence of air, since the discoloration rate is three times lower under nitrogen atmosphere. The decomposition of the indigoid dye is also sharply accelerated in the presence of Rose Bengal or of sizable quantities of acetone. This ketone was chosen, because it was already found to be an excellent sensitizer [9]: it has a high triplet energy (79–82 kcal mol^{-1}), so that upon irradiation, the triplet acetone is able to transfer its energy to dye molecules or to molecular oxygen (whose triplet energy is 22.5 kcal mol^{-1}). However, the fact that under nitrogen, the rate is only reduced by a factor of three suggests either a relatively efficient competing radical pathway.

Finally, UV irradiation can cause a complete discoloration of the solution. Nevertheless, irradiation times required to obtain a clean solution are prohibitive. Consequently, 253.7 nm-irradiation alone cannot be used as an effective procedure for removal of AB74 from water.

3.2. UV (253.7 nm)/H_2O_2 process

Whereas azo and anthraquinone dyes are resistant to discoloration with hydrogen peroxide [10], AB74 has proven to be sensitive to H_2O_2 in the absence of irradiation, even at room temperature [7]. But, once again, the disadvantage of this technique is that reaction times are very long. If hydrogen peroxide is applied simultaneously with UV irradiation, there is a drastic increase in the destruction rate of *the* dye when compared with the degradation rates achieved through the use of only one application, as illustrated on Fig. 1. This can be related to the production of hydroxyl radicals, a powerful oxidizing agent. Therefore, the rate of disappearance of AB74 is given by Eq. (3), assuming that $HO^{\bullet}$-induced oxidation is controlled by second-order kinetics (note that both photochemical (UV alone) and thermal processes are neglected).

$$-\frac{\mathrm{d[AB74]}}{\mathrm{d}t} = k_{\mathrm{HO}^{\bullet}}[\mathrm{HO}^{\bullet}][\mathrm{AB74}] \quad (3)$$

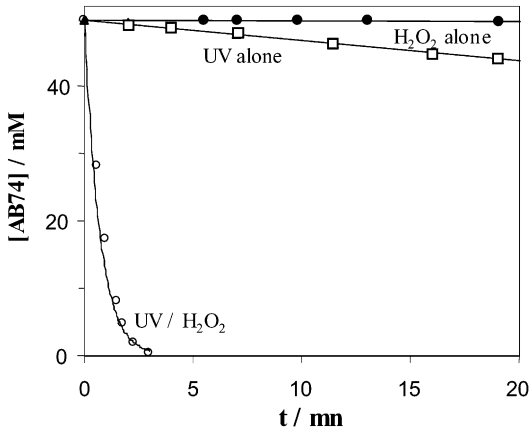

Fig. 1. Comparative evolution of the dye concentration vs. time for the UV, H_2O_2, and UV/H_2O_2 processes. $[AB74]_0 = 5 \times 10^{-5}$ M; $[H_2O_2]_0 = 2 \times 10^{-1}$ M; UV 253.7 nm; natural pH; 500 ml treated.

3.2.1. Apparent reaction order

In all experiments, a large excess of hydrogen peroxide with respect to the dye was added to the solution in order to maintain the concentration in hydroxyl radicals constant. The photooxidation is then expected to obey pseudo-first-order kinetics. Our results indicate that this only applies in very dilute solutions ($[AB74]_0 \approx 1.9 \times 10^{-5}$ M). Surprisingly, it is not appropriate at all at higher contents of pollutant (Fig. 2). Indeed, when $[AB74]_0 > 1.5 \times 10^{-4}$ M, the concentration of the dye decreases linearly with time (insert Fig. 2). It is noteworthy that such apparent zero-order kinetics in *homogeneous* systems is not frequently reported in the literature.

3.2.2. Influence of operational conditions on the treatment efficiency

3.2.2.1. Effect of the initial dye concentration. Moreover, through this study, it became evident that the

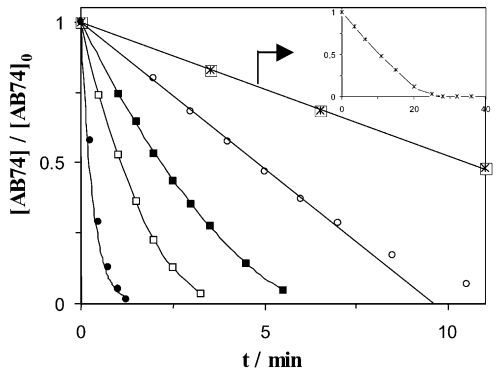

Fig. 2. Evolution of the dye concentration vs. time during the hydroxyl radical-induced oxidation. $[H_2O_2]_0 = 2 \times 10^{-1}$ M; UV 253.7 nm; natural pH; 500 ml treated $[AB74]_0 \times 10^4 = 5.0$ M (∗); 2.4 M (○); 1.5 M (■); 0.8 M; 0.19 M (●). Insert: disappearance of the dye AB74 at an initial concentration of 5×10^{-4} M on a longer time scale. $[H_2O_2]_0 = 2 \times 10^{-1}$ M; UV 253.7 nm; natural pH; 500 ml treated.

photodegradation rate depends on $[AB74]_0$. It must be kept in mind that as the lifetime of hydroxyl radicals is very short (only few nanoseconds), they can only react where they are formed. Increasing the quantity of AB74 molecules per volume unit logically enhances the probability of collision between organic matter and oxidizing species, leading to an increase in the discoloration rate. However, the molar extinction coefficient of the dye at 253.7 nm is very high ($18.7 \times 10^3\,\mathrm{l\,mol^{-1}\,cm^{-1}}$), so that a rise in its concentration induces an inner filter effect, i.e. incident light would largely be wasted for dye excitation rather than for the hydroxyl radical precursor excitation. Consequently, the solution becomes more and more impermeable to UV radiations. As the rate of hydrogen peroxide photolysis directly depends on the fraction of incident light absorbed by H_2O_2 molecules, the discoloration rate slows down. In fact, both above-mentioned opposing phenomena are responsible for the shape of the curve representing the initial discoloration rate versus $[AB74]_0$, namely for the presence of a maximum reaction rate, as illustrated on Fig. 3.

3.2.2.2. Effect of the initial hydrogen peroxide concentration. Moreover, the discoloration rate should be influenced by the hydrogen peroxide/AB74 molar ratio. Indeed, once again, two opposing factors must be considered:

1. If large quantities of H_2O_2 are added to the solution, the fraction of light absorbed by the photo-decomposition promoter and consequently its photolysis rate increase. More hydroxyl radicals are available for the dye oxidation.
2. $HO^\bullet$ radical efficiently reacts with hydrogen peroxide (Eq. (5)), so that H_2O_2 in excess contributes to the $HO^\bullet$-scavenging capacity and reduces the efficiency of pollutant degradation [11].

$$H_2O_2 + h\nu \rightarrow 2HO^\bullet \tag{4}$$

$$H_2O_2 + HO^\bullet \rightarrow HO_2^\bullet + H_2O, \quad k = 2.7 \times 10^7\,\mathrm{M^{-1}\,s^{-1}} \tag{5}$$

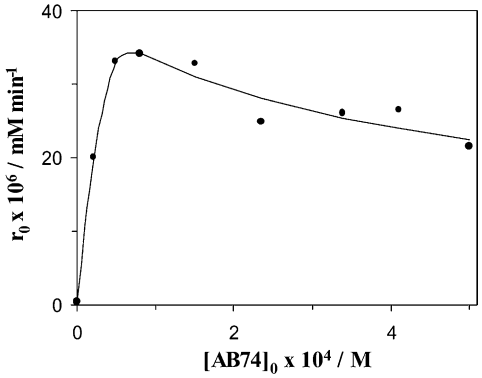

Fig. 3. Influence of the initial dye concentration on the discoloration rate r_0. $[H_2O_2]_0 = 9.7 \times 10^{-2}$ M; UV 253.7 nm; natural pH; 500 ml treated.

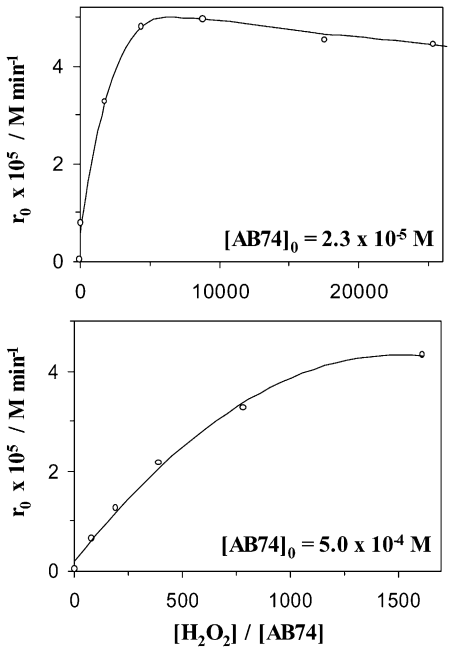

Fig. 4. Influence of the initial concentration in hydrogen peroxide on the discoloration rate r_0: 253.7 nm; natural pH; 500 ml treated.

Additional experiments (Fig. 4) confirm this assumption. For instance, when $[AB74]_0 = 2.3 \times 10^{-5}$ M, increasing hydrogen peroxide concentration induces a drastic rise in the reaction rate r_0 up to $4.96 \times 10^{-5}\,\mathrm{M\,min^{-1}}$. When the H_2O_2/AB74 ratio is higher than 5000, r_0 drops. The second factor (2) is predominant.

Note that $HO_2^\bullet$ radicals are less reactive than $HO^\bullet$, with reaction rate constants lower than $2 \times 10^4\,\mathrm{M^{-1}\,s^{-1}}$ in the presence of organic matter [12], leading therefore to negligible contribution in the dye degradation.

3.2.2.3. Effect of the initial pH. Previous experiments were systematically carried out at an initial pH of 4.4, the natural one. Nevertheless, with a view to an industrial use of the process, the operational conditions must be optimized. The pH was made more acidic by adding four inorganic acids: HCl, HNO_3, H_3PO_4 and H_2SO_4. The four counterions A^{x-} have qualitatively the same influence on the initial rate, leading roughly to a bell-shaped curve. Indeed, r_0 increases slightly up to pH $\approx$ 2–2.5, and decreases significantly at lower pH values, as illustrated on Fig. 5. Similar results have already been reported for azo dyes [13,14].

Concomitant with the acidification of the solution, increasing amounts of conjugated base were added to the solution. Now, the anions A^{x-} are able to react with hydroxyl radicals leading to inorganic radical ions. These inorganic radical anions show a much lower reactivity than $HO^\bullet$, so that they do not take part in the dye decomposition. There is also a drastic competition between the dye and anions with respect to $HO^\bullet$. However, even in the most defavourable case, i.e. at pH = 1.5 and in the presence of chloride ions

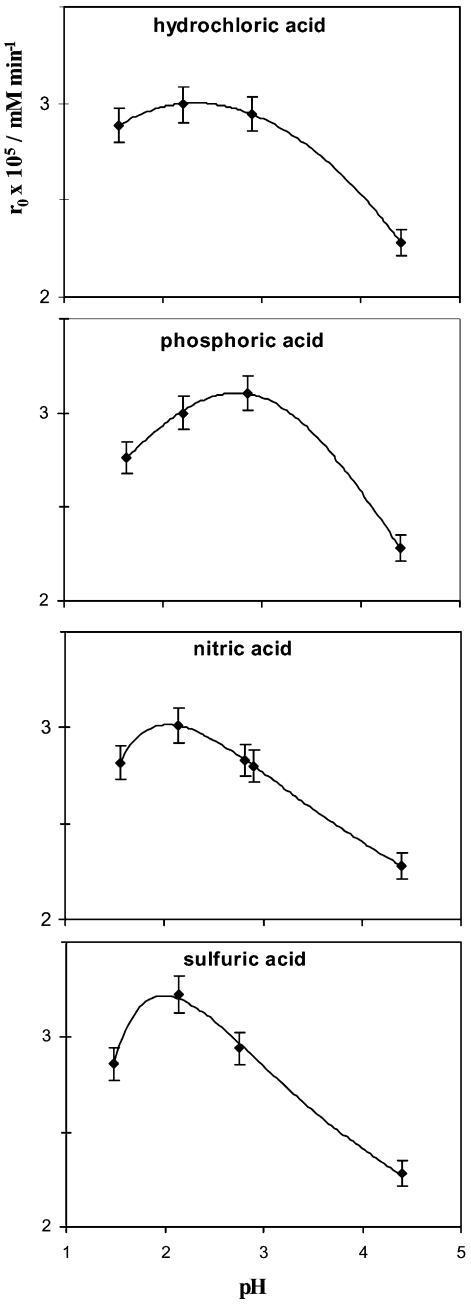

Fig. 5. Effect of pH on the rate of discoloration of the dye solution. $[AB74]_0 = 5 \times 10^{-4}$ M; $[H_2O_2]_0 = 2 \times 10^{-1}$ M; UV 253.7 nm; 500 ml treated.

($k = 4.3 \times 10^9\,M^{-1}\,s^{-1}$, Eq. (6)), at least 6% of $HO^\bullet$ radicals react with AB74, since the rate constant for the reaction between hydroxyl radicals and dye molecules is very high ($1.8 \times 10^{10}\,M^{-1}\,s^{-1}$, according to Sychev et al. [15]). And this is sufficient for the photochemical degradation to be effective.

The evolution in very acidic solutions cannot be exclusively correlated with this scavenging effect of A^{x-} toward $HO^\bullet$ radicals. Indeed, a comparison of the efficiency of the process at optimal pH and at pH = 1.5 suggests that the eventual increasing scavenging effect is: chloride < phosphate < nitrate < sulfate, which is not in agreement with the values of the rate constants obtained in the literature for the reaction between $HO^\bullet$ and the above-mentioned anions [16–19].

$$Cl^- + HO^\bullet \rightarrow ClOH^{\bullet -}, \quad k = 4.3 \times 10^9\,M^{-1}\,s^{-1} \tag{6}$$

$$NO_3^- + HO^\bullet \rightarrow NO_3^\bullet + H_2O, \quad k = 1.3 \times 10^8\,M^{-1}\,s^{-1} \tag{7}$$

$$HSO_4^- + HO^\bullet \rightarrow SO_4^{\bullet -} + H_2O, \quad k = 4.7 \times 10^5\,M^{-1}\,s^{-1} \tag{8}$$

$$H_2PO_4^- + HO^\bullet \rightarrow HPO_4^{\bullet -} + H_2O, \quad k \approx 2 \times 10^4\,M^{-1}\,s^{-1} \tag{9}$$

It can be postulated that AB74, with two sulfonic groups, gives rise in pure water to single anions and shows only low tendency to aggregate. However, this aggregation is largely promoted by the presence of strong electrolytes, especially sulfuric acid (which induces the largest decrease in the reaction rate during our investigation). Moreover, addition of such electrolytes, even in small amounts, causes a marked reduction on the diffusion coefficient of the organic matter. Now, aggregates of two or three molecules are less accessible to hydroxyl radicals than single molecules.

Finally, dye content, initial hydrogen peroxide concentration and pH are important parameters, which govern the discoloration rate. At the industrial stage, it is not straightforward to define optimal conditions. However, the present results show that the process should rather be performed at a pH close to 2–3. Industrialists will be well-advised to dilute their aqueous effluents to decrease the absorbance of the solution and to add at least 2–3% v/v of hydrogen peroxide 30% w/v.

3.2.3. Degradation mechanism

In a previous article [20], we demonstrated that, during the $UV/H_2O_2/O_2$ oxidation of hydroxyazo dyes, the absorbance drops to zero not only at the maximum absorption of the original compound, but also in the whole visible part of the spectrum at the same time. In the case of AB74, the initial blue coloration disappears rapidly. However, the solution is not discolored. It changes from blue to orange-colored due to the formation of intermediates containing a chromophoric group. Indeed, a new band appears in the 480–570 nm region, centered at 513 nm. The absorbance at 513 nm reaches a maximum close to the end of the bleaching period and is brought eventually to zero by continuing irradiation. Under nitrogen atmosphere, the absorbance is still growing in the 480–570 nm area, but another band is detected at higher wavelengths (with a maximum at about 660 nm). The corresponding product is more conjugated that the original dye. It

is probable that AB74 undergoes hydroxylation. Dimerisation of two organic radicals is also possible. Moreover, even if the blue coloration disappears more quickly in air than under nitrogen atmosphere, in the latter case, a complete decomposition of AB74 molecules can still be achieved. From this experiment, it can be deduced that breaking of the original dye does not necessarily require O_2.

Literature indicates that upon chemical oxidation, for instance by ozonation [21], the ethylenic bond of indigo is broken, leading to isatin. In order to check the possible formation of isatinsulfonic acid during $HO^{\bullet}$-induced oxidation of AB74, photolysis of a standard solution was conducted, in the presence of hydrogen peroxide, in deuterium oxide. Products of the dye degradation were examined by ^1H NMR spectroscopy. The resulting spectra, represented on Fig. 6, were recorded after various irradiation times (0, 3 h 15, 4 h 30 and 10 h).

On spectrum (β), which corresponds to a yellow solution, disappearance of signals situated at 6.6, 7.6 and 7.9 ppm, which are the fingerprint of AB74, indicates the complete elimination of the original dye. However, the latter is not fully mineralized, since many peaks are still detected

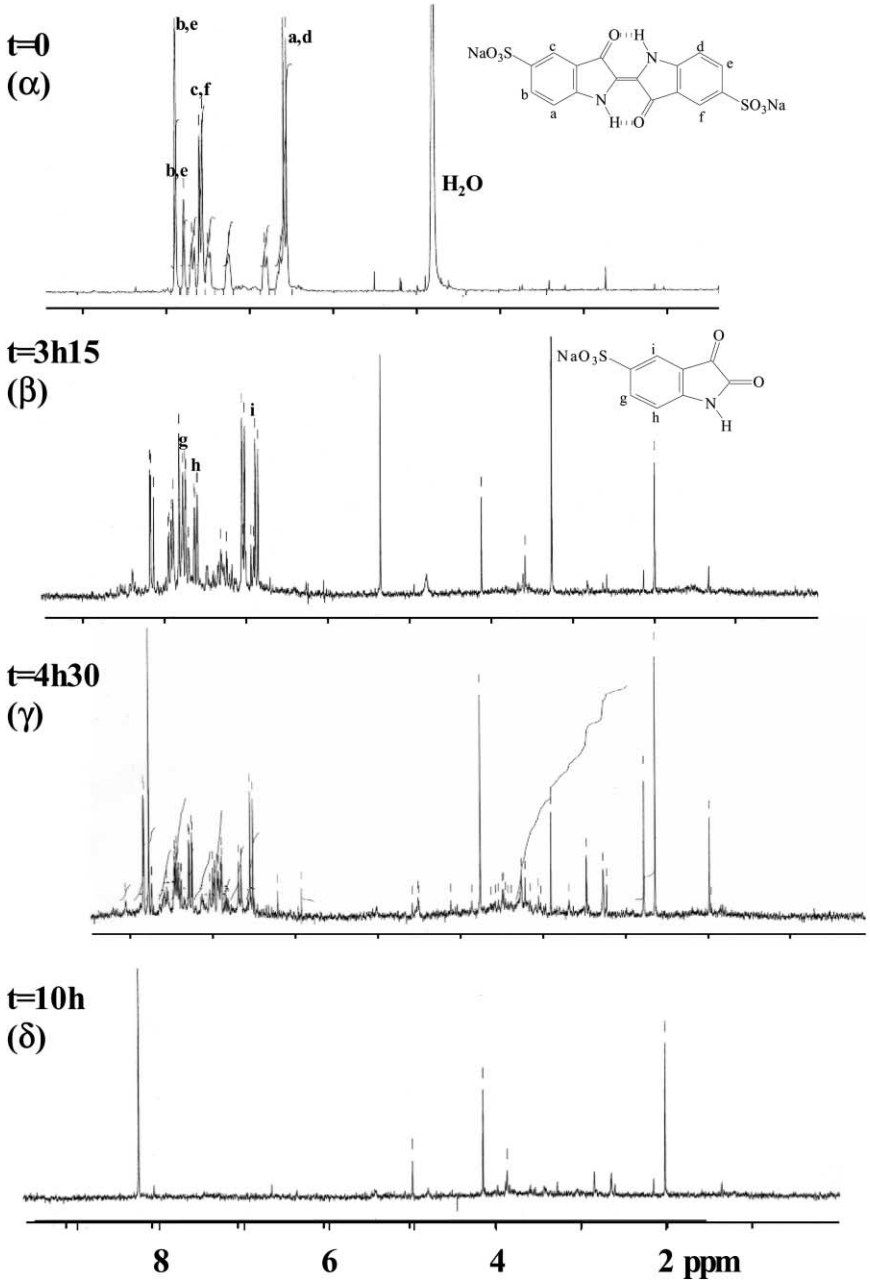

Fig. 6. ^1H NMR spectra of AB74 before irradiation and after various treatment times (solvent: D_2O). $[AB74]_0 = 4 \times 10^{-3}$ M; $[H_2O_2]_0 = 1.9$ M; UV 253.7 nm; natural pH; 1 ml treated.

between 9 and 7 ppm. The presence of such signals, clearly different in nature and distribution than in spectrum (α), is a proof of a non-destructive modification of the aromatic rings. It is worth noting that multiplets at 7.0, 7.7 and 7.8 ppm actually correspond to isatinsulfonic acid (ISA). The additional signals also appear on the ^{1}H NMR spectrum of an incompletely photoreacted solution of ISA. This suggests that

1. ISA is the primary stable breakdown product during the UV/H_2O_2-induced oxidation of AB74. Consequently, the C=C double bond in AB74 is the most vulnerable part of the molecule toward $HO^\bullet$-induced oxidation.
2. ISA is converted into derivatives which carry deshielded protons (7–9 ppm), i.e. aromatic compounds. Their subsequent hydroxylation may explain the rise in the absorbance in the 480–570 nm region. Substitution of the sulfonate group by hydroxyl radical also occurs, since an hydroxylated benzoic acid was detected by GC/MS after esterification.

Signals are observed between 1.3 and 4.2 ppm on the ^{1}H NMR spectrum (β). They can be ascribed to hydrogen atoms carried by aliphatic compounds. The thin singlet at 8.2 ppm also detected on spectrum (γ) corresponds to a very deshielded proton. We are inclined to consider it to be due to formic acid [22]. Other multiplets relative to aliphatic intermediates are detected after a prolonged irradiation (spectrum δ). Sodium succinate and sodium malonate have actually been detected by GC/MS after derivatization. The production of such acids is also responsible for the drop of the pH of the solution from 4.4 to 2.5 during the treatment.

The complete disappearance of the signals of aromatic derivatives precisely coincides with the change in the solution coloration from yellow to colorless. Additional experiments showed that the transformation of benzenic compounds into aliphatic acids does not induce a large release of carbon dioxide. Indeed, the total organic carbon (TOC) is only reduced by 14% using $[AB74]_0 = 5 \times 10^{-4}$ M and $[H_2O_2]_0 = 4 \times 10^{-1}$ M at natural pH, at the end of the bleaching stage. However, this is not a real problem, since the ultimate aliphatic breakdown products are non toxic and biodegradable. Therefore, it can be concluded that the UV/H_2O_2 process may be, in the future, a good alternative to physical methods in use to discolor textile wastewaters.

3.3. Photocatalytic process

The use of semiconductors, such as TiO_2 and ZnO, as photocatalysts has being extensively studied [23–25] and the number of papers related to this topic increases tremendously. It has the large advantage over the UV/H_2O_2 method to allow application of cheap energy sources, such as artificial near-UV light or sunlight.

When a semiconductor is irradiated, electrons are excited from the valence to the conduction band, generating positive holes and free electrons. The energy gap between these bands is 3.05 eV (420 nm) in rutile and 3.2 eV (390 nm) in anatase. It is similar in zinc oxide. Electrons and holes can recombine or interact with other molecules. Indeed, electrons can be scavenged by oxygen. Positive holes oxidize organic substrates, anchored to the oxide surface, by direct electron transfer or react with electron donors in the solution to produce hydroxyl radicals. The overall process can be depicted by Eqs. (10)–(16).

$$TiO_2 + h\nu\,(UV) \rightarrow TiO_2\,(e^-_{CB}, h^+_{VB}) \quad (10)$$

$$TiO_2\,(e^-_{CB}, h^+_{VB}) \rightarrow TiO_2 + \text{Heat} \quad (11)$$

$$TiO_2\,(h^+_{VB}) + H_2O_{ads} \rightarrow TiO_2 + H^+ + OH^\bullet{}_{ads} \quad (12)$$

$$TiO_2\,(h^+_{VB}) + HO^-_{ads} \rightarrow TiO_2 + OH^\bullet{}_{ads} \quad (13)$$

$$O_2 + TiO_2\,(e^-_{CB}) \rightarrow TiO_2 + O_2{}^{\bullet -} \quad (14)$$

$$OH^\bullet{}_{ads} + \text{Dye} \rightarrow \text{Degradation of the dye} \quad (15)$$

$$h^+_{VB} + \text{Dye} \rightarrow \text{Dye}^{\bullet +} \rightarrow \text{Oxidation of the dye} \quad (16)$$

Under the experimental conditions explored in the present work, photooxidation rates ($r = -dC/dt$) on TiO_2 Degussa P25 are constant. This behavior is not rare in literature. It has already been reported during the photocatalytic degradation of salicylic acid and 3-chloro-4-hydroxybenzoic acid [26,27]. AB74 also disappears according to zero-order kinetics on TiO_2 Tiona PC 100 and Tiona PC 500, whereas kinetics can be described by a pseudo-first order with TiO_2 R900 and ZnO. With the catalyst TiO_2 TC4, neither first, nor zero order kinetics can explain the experimental concentration — time data. These different behaviors can be rationalized in terms of modified forms of the Langmuir–Hinshelwood treatment, which underlines the key role of the adsorption constant K on kinetics, assuming that adsorption — desorption kinetics is faster than the photochemical reaction. Indeed, the rate of unimolecular surface reaction, r_{LH}, is proportional to the surface coverage, supposing that the reactant is more strongly adsorbed on semiconductor particules than the products

$$r_{LH} = -\frac{dC}{dt} = \frac{kKC}{1 + KC} \quad (17)$$

with C is the concentration in the dye at time t; k the second order rate constant ($M^{-1}\,s^{-1}$); K the adsorption constant ($mol\,l^{-1}$).

The integrated form of (17) is

$$t = \frac{1}{Kk}\ln\frac{C_0}{C} + \frac{1}{k}(C_0 - C) \quad (18)$$

The extent of adsorption of AB74 on Degussa P25 TiO_2 particles at pH = 5.6 was measured monitoring the solute concentration in the bulk solution before and after the adsorption–desorption equilibrium was reached. The adsorption constant K was evaluated at $1.3 \times 10^5\,l\,mol^{-1}$. In that case, the first term of expression (18) becomes small

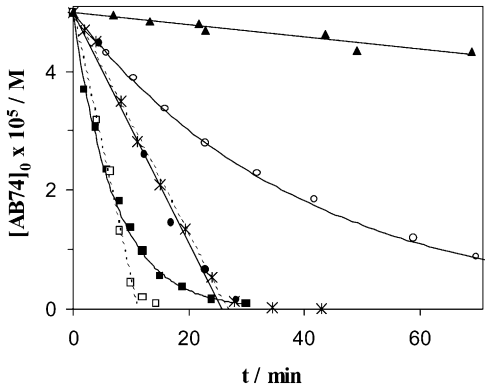

Fig. 7. Influence of the nature of the catalyst on the discoloration order. $[AB74]_0 = 5 \times 10^{-5}$ M; catalyst = 0.6 g l^{-1}; natural pH; 500 ml treated.

compared with the second one and under these conditions, $C - C_0 \approx -kt$. The concentration of the dye decreases linearly with irradiation time. On the contrary, AB74 molecules are weakly anchored on ZnO with $K_{ZnO} = 1.6 \times 10^4$ l mol^{-1}, so that the first term of Eq. (18) is predominant. Then $\ln(C_0/C) \approx kKt = k't$. On the other hand, $K_{TiO_2TC4} = 4.9 \times 10^4$ l mol^{-1}, so that both contributions must be taken into account. Finally, the surface ability of absorbing substrates is an important parameter, which governs the apparent reaction order.

To compare the photocatalytic activities of different catalysts, degradations were carried out using slurries containing 0.6 g l^{-1} of TiO_2 or ZnO and an initial dye concentration of 23.4 mg l^{-1}. Results also indicate that TiO_2 P25, TiO_2 Tiona PC 100, TiO_2 Tiona PC 500, with a predominant anatase crystalline phase, and ZnO are effective catalysts for the degradation of AB74, whereas rutile TiO_2 R900 and TiO_2 TC4 do not efficiently induce the oxidation of the dye, as illustrated on Fig. 7. Consequently, the catalytic ability of titanium dioxide is dramatically dependent on its crystalline form. However, the reasons for the quantitative differences between the photocatalytic activities of rutile and anatase are not really transparent. From the thermodynamical point of view, photooxidation should occur with the same efficiency for both anatase and rutile. But it has been reported that despite the greater free-carrier mobility in anatase, the surface recombination of photoexcited electron and positive holes is higher in rutile [28–30]. Moreover, a range of photoactivities are observed for each polymorph. This suggest that variables such as crystal and particule sizes, manufacturing route (temperature, heating time) give rise to subtle changes in activity. Edge et al. [31] add that samples of mixed morphology (TiO_2 P25 in the present case) are generally the most photoactive. These authors postulated that electrons produced in anatase microcristallites quickly diffuse to become localized in rutile regions.

It is worth noting that a rapid discoloration is achieved with zinc oxide as the catalyst. However, on the industrial point of view, it is crucial to remember that ZnO would not

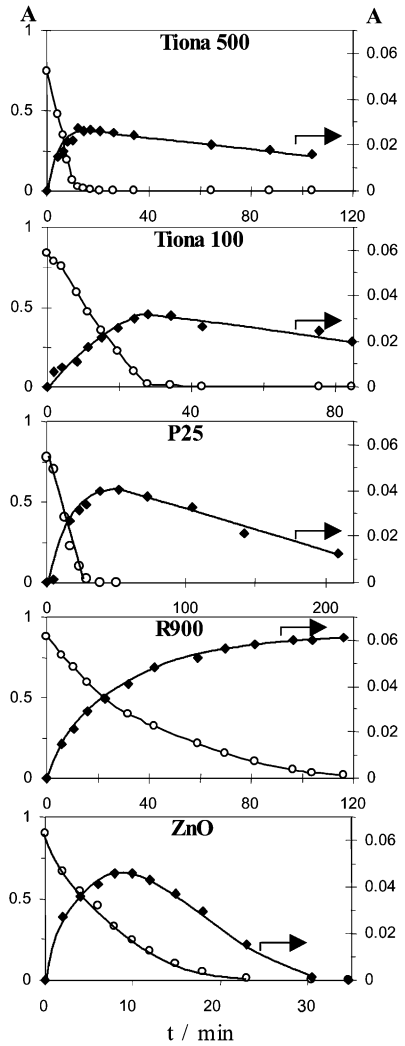

Fig. 8. Evolution of the absorbance at 609 (○) and 409 nm (◆) during the photocatalytic degradation of AB74. $[AB74]_0 = 5 \times 10^{-5}$ M; catalyst = 0.6 g l^{-1}; natural pH; 500 ml treated.

be an efficient catalyst, since it can only be used in neutral or alkaline media. This is not compatible with the pH of most dyehouse wastewaters.

3.3.1. Degradation mechanism

Formation and disappearance of aromatic yellow intermediates were evaluated by monitoring the evolution of the absorbance at 409 nm during the treatment. It seems that the amount of breakdown-products vary with the nature of the photocatalyst. Increasing quantities are obtained, as follows: TiO_2 Tiona PC 500 < TiO_2 Tiona PC 100 < TiO_2 P25 < TiO_2 R900. This phenomenom may correspond to a variation in the reaction mechanism. But it may also be ascribed to the difference in the total surface exposed. If by-products have an important adsorption constant, photocatalysts with a large surface area would probably readsorb more organic intermediates as soon as they appear in the solution. Nevertheless, whatever the

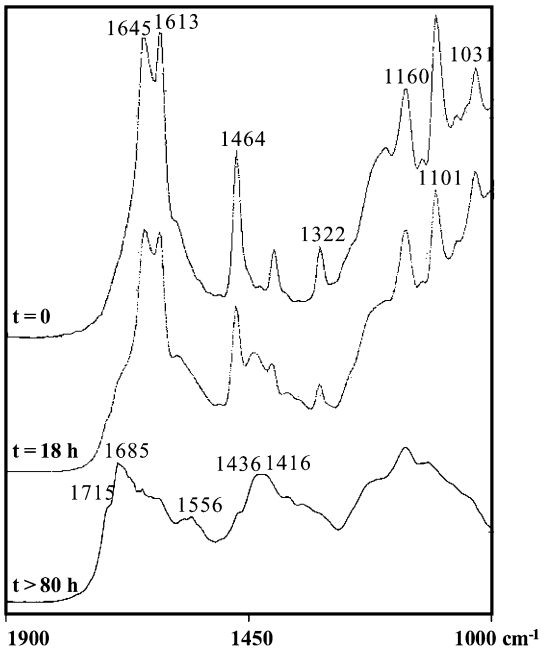

Fig. 9. FTIR spectra of AB74 adsorbed on TiO_2 P25 after increasing irradiation times.

catalyst, the accumulation reaches a maximum when the original pollutant is just decomposed. With ZnO, lifetimes of the aromatic intermediates are shorter; they do not exceed that of the original dye, as illustrated on Fig. 8.

^{1}H NMR and FTIR spectroscopies were used to gain informations about the nature of degradation products. Experiments were performed with TiO_2 P25. FTIR spectra for the photodegraded AB74 on TiO_2 P25 are presented on Fig. 9. The band intensities of the alkene bond (1615 cm^{-1}) and of the aromatic moieties (C=C at 1639, and 1475 cm^{-1}) decreased with irradiation time. This is the sign of the disappearance of the original pollutant and of its primary benzenic breakdown products. Simultaneously, there is a collapse of the absorbance in the range 1000–1250 cm^{-1}, which corresponds to the disappearance of stretching vibrations in sulfonate groups. Moreover, after prolonged irradiation, bands due to oxalates (1714, 1690 cm^{-1}), formats (1570, 1560, shoulders near 1385 and 1355 cm^{-1}) [32], and to an interaction between the C–O stretching and the O–H bending in a carboxylic acid, probably acetic acid (1416 cm^{-1}), are apparent [33]. Production of sizable quantities of formic acid was confirmed by ^{1}H NMR analysis. It is noteworthy that no traces of isatinsulfonic acid could be detected by both techniques.

4. Conclusion

During this work, both UV/H_2O_2 and UV/TiO_2 processes proved to be powerful in destroying the indigoid dye AB74. For the homogeneous system, the following conclusions can be drawn:

1. The dye AB74 is very sensitive to oxidation, and its discoloration rate strongly depends on operating conditions, i.e. dye content, hydrogen peroxide concentration and pH.
2. The dye AB74 is quickly converted into colored aromatic intermediates, including isatinsulfonic acid, which react rather slowly with hydroxyl radicals.
3. After prolonged irradiation time, only aliphatic acids can be detected by GC and ^{1}H NMR techniques.

For the heterogeneous system, the kinetic model of Langmuir–Hinshelwood describes well the photoreactivity results obtained with various commercially available catalysts. Their crystalline form and their surface ability of absorbing substrates are important parameters that govern the apparent reaction order kinetics. From the mechanistic viewpoint, it was shown, using ^{1}H NMR and FTIR spectroscopies, that AB74 molecules undergo irreversible oxidation, leading to non toxic and biodegradable ultimate breakdown products, such as formic, acetic, oxalic acids.

Further studies on the practical use of photocatalysis and photochemical treatment should involve formulated dyes in order to carry out experiments that better reflect the *actual* water pollution conditions.

References

[1] M.L. Richardson, J. Soc. Dyers. Colour. 99 (1983) 198.
[2] P. Cooper, J. Soc. Dyers. Colour. 109 (1993) 97.
[3] Uygur, J. Soc. Dyers Colorists 113 (1997) 211.
[4] O. Legrini, E. Oliveros, A.M. Braun, Chem. Rev. 93 (1993) 671.
[5] C. Galindo, A. Kalt, J. Adv. Oxid. Technol., in press.
[6] L.M. Camerero, R. Peche, A. Collado, Int. J. Chem. Kinetics 29 (1997) 575.
[7] G. Shama, D.W. Drott, Chem. Eng. Commun. 158 (1997) 107.
[8] N. Kuramoto, T. Kitao, J. Soc. Dyers Colorists (1979) 257.
[9] C.P.C. Poon, B.M. Vittimberga, Ind. Waste. Proc. Mid-Atl. Conf. 13 (1981) 427.
[10] C.G. Namboodri, W.K. Walsh, Am. Dyestuff Reporter (1995) 86.
[11] H. Christensen, K. Sehested, H. Corfitzen, J. Am. Chem. Soc. 86 (1982) 1588.
[12] A.D. Nadezhdin, H.B. Dunford, Can. J. Chem. 57 (1979) 3017.
[13] C. Galindo, A. Kalt, Dyes Pigments 40 (1998) 27.
[14] H.-Y. Shu, C.-R. Huang, M.-C. Chang, Hazard. Ind. Wastes 26 (1994) 186.
[15] Ya. Sychev, V.G. Isak, U. Pfannmeller, Russ. J. Phys. Chem. 53 (1979) 1595.
[16] G.G. Jayson, B.J. Parsons, A.J. Swallow, J. Chem. Soc., Faraday Trans. 1 69 (1973) 1597.
[17] Y. Katsumura, P.Y. Jiang, R. Nagaishi, T. Oishi, K. Ishigura, Y. Yoshida, J. Phys. Chem. 95 (1991) 4435.
[18] P.-Y. Jiang, Y. Katsumura, R. Nagaishi, M. Domae, K. Ishikawa, K. Ishigura, Y. Yoshida, J. Chem. Soc., Faraday Trans. 1 88 (1992) 1653.
[19] P. Maruthamuthu, P. Neta, J. Phys. Chem. 82 (1978) 710.
[20] C. Galindo, P. Jacques, A. Kalt, J. Adv. Oxid. Technol. 4 (1999) 400.
[21] K. Takeuchi, T. Takashi, Anal. Chem. 61 (1989) 619.
[22] C. Galindo, P. Jacques, A. Kalt, J. Photochem. Photobiol. A Chem. 130 (2000) 35.

[23] M.R. Hoffmann, S.T. Martin, W. Choi, D.W. Bahnemann, Chem. Rev. 95 (1995) 69.
[24] C. Richard, F. Bosquet, J.-P. Pilichowski, J. Photochem. Photobiol. A Chem. 108 (1997) 45.
[25] W.Z. Tang, H. An, Chemosphere 31 (1995) 4157.
[26] J. Cunningham, G. Al-Sayyed, J. Chem. Soc. Faraday Trans. 86 (1990) 3935.
[27] A.E. Regazzoni, P. Mandelbaum, M. Matsuyishi, S. Sciller, S.A. Bilmes, M.A. Blesa, Langmuir 14 (1998) 868.
[28] G. Dagan, M. Tomkiewicz, J. Phys. Chem. 97 (1993) 12651.
[29] A. Sclafani, L. Palmisano, M. Schiavello, J. Phys. Chem. 94 (1990) 829.
[30] B. Ohtani, S. Zhang, J. Handa, H. Kajiwara, S. Nishimoto, T. Kagiya, J. Photochem. Photobiol. A: Chem. 64 (1992) 223.
[31] M. Edge, R. Janes, J. Robinson, N. Allen, F. Thompson, J. Warman, J. Photochem. Photobiol. A: Chem. 113 (1998) 171.
[32] G. Busca, J. Lamotte, J.-C. Lavalley, V. Lorenzelli, J. Am. Chem. Soc. 109 (1987) 5197.
[33] J.M. Gallardo Amores, V. Sanchez Escribano, R. Gianguido, G. Busca, Appl. Catal. B: Environ. 13 (1997) 45.